QUARTERLY OF APPLIED MATHEMATICS
VOLUME LXXV, NUMBER 4
DECEMBER 2017, PAGES 769–782
http://dx.doi.org/10.1090/qam/1469
Article electronically published on March 10, 2017

MATHEMATICAL MODEL AND ANALYSIS OF THE STRENGTH OF PARTICLE REINFORCED IDEALLY PLASTIC COMPOSITES

By

GUILLERMO H. GOLDSZTEIN

School of Mathematics, Georgia Institute of Technology, 686 Cherry Steert, Atlanta, Georgia 30332-0160

Abstract. We consider fiber reinforced ideally plastic composites. We analyze a mathematical model valid for microstructures and applied stresses that lead to both microscopic and macroscopic anti-plane shear deformations. We obtain a bound on the yield set of the reinforced material in terms of the shapes of the cross section of the fibers, their volume fraction, and the yield stresses of the matrix. We construct examples showing that our bound is sharp.

1. Introduction. The stresses that an ideally plastic material can withstand form a bounded closed set $\bar{\mathcal{Y}}$ in the space of symmetric 3×3 real matrices. The set $\bar{\mathcal{Y}}$, which is a material property, is called the yield set or strength domain. Unlike brittle materials, ideally plastic materials do not break. When subjected to a stress that is in the boundary of $\bar{\mathcal{Y}}$, the material experiences a permanent deformation, usually called plastic deformation.

Fiber-reinforced composites are materials made of strong fibers embedded in a weaker material referred to as the matrix. In this article, we will consider fiber-reinforced composites where both the matrix and fibers are ideally plastic materials.

We denote by $\bar{\mathcal{Y}}_{\mathrm{f}}$ the yield set of the material the fibers are made of, and by $\bar{\mathcal{Y}}_{\mathrm{m}}$ the yield set of the matrix. Thus, the stresses within the fibers are restricted to the set $\bar{\mathcal{Y}}_{\mathrm{f}}$ but within the matrix the stresses are restricted to the set $\bar{\mathcal{Y}}_{\mathrm{m}}$. In mathematical terms, if we denote by Ω the region in space occupied by the composite, and for each $\mathbf{x} \in \Omega$ we define

$$\bar{\mathcal{Y}}_{\mathbf{x}} = \begin{cases} \bar{\mathcal{Y}}_{\mathrm{f}} & \text{if } \mathbf{x} \text{ is in a fiber,} \\ \bar{\mathcal{Y}}_{\mathrm{m}} & \text{if } \mathbf{x} \text{ is in the matrix,} \end{cases} \tag{1}$$

Received August 16, 2016 and, in revised form, February 14, 2017.
2010 *Mathematics Subject Classification.* Primary 74C05, 74Q05, 74Q15, 74Q20.
Key words and phrases. Microstructures, yield condition, fiber-reinforced composite material, ideally plastic material, variational calculus.
E-mail address: ggold@math.gatech.edu

then, if the composite is subject to a stress $\bar{\sigma}$ that may vary within the material $\bar{\sigma} = \bar{\sigma}(\mathbf{x})$, we have

$$\bar{\sigma}(\mathbf{x}) \in \bar{\mathcal{Y}}_{\mathbf{x}}, \tag{2}$$

for all $\mathbf{x} \in \Omega$.

We will only consider time independent stresses $\bar{\sigma}$ and thus, $\bar{\sigma}$ also satisfies the equilibrium equations

$$\nabla \cdot \bar{\sigma} = 0, \tag{3}$$

where $\nabla \cdot \bar{\sigma}$ is the divergence of $\bar{\sigma}$.

Loosely speaking, the microstructure or microgeometry of the composite refers to the description of the regions in space occupied by the fibers and the matrix. Mathematically speaking, the microstructure is determined by the function $\mathbf{x} \mapsto \bar{\mathcal{Y}}_{\mathbf{x}}$.

Assume the microstructure $\bar{\mathcal{Y}}_{\mathbf{x}}$ is periodic with period cell $\bar{Q}$, where $\bar{Q}$ is a parallelepiped. A stress field $\bar{\sigma}$ is said to be admissible if it is $\bar{Q}$-periodic and satisfies the restrictions (2) and the equilibrium equations (3).

In the limit in which the size of the period cell $\bar{Q}$ is much smaller than the size of the material, the fiber reinforced composite behaves *macroscopically* as a homogeneous material that can withstand only the stresses that belong to the set $\bar{\mathcal{Y}}_{\text{hom}}$ defined by

$$\bar{\mathcal{Y}}_{\text{hom}} = \{\bar{\tau} : \bar{\tau} = \langle \bar{\sigma} \rangle, \text{ for some } \bar{\sigma} \text{ admissible}\}, \tag{4}$$

where $\langle \bar{\sigma} \rangle$ is the average of $\bar{\sigma}$, i.e., $\langle \bar{\sigma} \rangle = |\bar{Q}|^{-1} \int_{\bar{Q}} \bar{\sigma}(\mathbf{x})\, \mathrm{d}\mathbf{x}$ with $|\bar{Q}|$ being the volume of $\bar{Q}$. In colloquial words, $\bar{\mathcal{Y}}_{\text{hom}}$ is the set of *macroscopic* stresses that the composite can withstand. We will refer to $\bar{\mathcal{Y}}_{\text{hom}}$ as the yield set of the composite. The justification of equation (4) is a well understood fact of the theory of mathematical homogenization. We refer the reader to [3, 10, 23, 29] for details.

In practice, all the details of the microstructure $\bar{\mathcal{Y}}_{\mathbf{x}}$ are not known or cannot be controlled. Instead, only some partial information, such as the volume fraction of the fibers, is available. Accordingly, the general objective in the mathematical study of these type of materials has been to obtain bounds or estimates on $\bar{\mathcal{Y}}_{\text{hom}}$, the set of stresses the composite can withstand, in terms of the yield sets of the matrix and the fibers, and information that may be available about the microstructure. This is also our goal in this article.

Fiber-reinforced composites, where both the fibers and the matrix are (to a good approximation) ideally plastic, are very important and widely used in applications. Thus, their study, both theoretical and experimental, is a very active field of research.

From the mathematical point of view, fiber-reinforced composites belong to the wider class of materials known as heterogeneous solids, which include composites and polycrystals. The same mathematical tools are sometimes used to study different heterogeneous solids. Ideally plastic materials are highly non-linear. Nevertheless, heterogeneous materials made of ideally plastic pure phases (the fibers and the matrix in our case) have proved to be amenable to detailed mathematical analysis. Thus, their study is very appealing since it can serve to test the existing mathematical methods, to develop new ones, and to gain intuition on the behavior of real materials. For the reasons mentioned

in this and the previous paragraphs, the literature on the mathematical study of heterogeneous materials made of ideally plastic pure phases is very extensive. Some examples include [2, 4, 5, 7, 13–15, 19, 21, 28, 30]. Examples of related non-linear homogenization problems include [1, 25, 31].

In our work, we will study the effect of the fiber shape on the yield set of the composite in the scalar two-dimensional problem that results from restricting our attention to applied stresses and microstructures that lead to both *microscopic* and *macroscopic* anti-plane shear. We first derive a bound on the yield set of the composite, and then construct examples of composites showing that our bound is essentially optimal.

We mention that, while our results are new, the yield set of fiber- or particle-reinforced composites has been a subject extensively studied [6, 8, 9, 11, 16, 20, 22, 24].

Our bound can be considered to be an application of a mathematical technique known as the translation method [18, 26, 27]. Other examples where the translation method was used to study non-linear composites or polycrystals include [12, 15, 17]. Particularly, the work in [15] has motivated a lot of work in this area of research.

This article is organized as follows: In Section 2 we reduce the original three-dimensional vectorial problem to a two-dimensional scalar problem by considering applied stresses and microstructures that lead to both microscopic and macroscopic anti-plane shear deformations. In Section 3 we derive our bound on the *strength* of the weakest direction of the composites we consider. In Section 4 we analyze the case when the cross section of the fibers are circular. In Section 5 we study composites with fibers with slender cross sections. In Section 6 we show that our bound (in a sense specified in that section) is sharp. We conclude with some discussions in Section 7.

2. The microstructures and anti-plane shear.

2.1. *The microstructures and the yield sets of the pure phases.* As usual, we denote by x_1, x_2 and x_3 the components of the position vector $\mathbf{x}$, i.e., $\mathbf{x} = (x_1, x_2, x_3)$. We assume that the fibers are parallel to the x_3-axis and the cross sections of the fibers (intersection of a fiber with a plane of the form $x_3 = \text{constant}$) are independent of x_3. In other words, the function $\mathbf{x} \mapsto \bar{\mathcal{Y}}_{\mathbf{x}}$ is independent of x_3. Note that, as a consequence, the period cell $\bar{Q}$ is of the form $\bar{Q} = Q \times [a, b]$, where Q is a parallelogram in $\mathbb{R}^2$ and a and b are any numbers that satisfy $a < b$.

We also assume that the yield sets $\bar{\mathcal{Y}}_{\mathrm{f}}$ and $\bar{\mathcal{Y}}_{\mathrm{m}}$ are convex sets with the following symmetric property: For both $\bar{\mathcal{Y}} = \bar{\mathcal{Y}}_{\mathrm{f}}$ and $\bar{\mathcal{Y}} = \bar{\mathcal{Y}}_{\mathrm{m}}$,

$$\text{if } \begin{bmatrix} \bar{\sigma}_{11} & \bar{\sigma}_{12} & \bar{\sigma}_{13} \\ \bar{\sigma}_{21} & \bar{\sigma}_{22} & \bar{\sigma}_{23} \\ \bar{\sigma}_{31} & \bar{\sigma}_{32} & \bar{\sigma}_{33} \end{bmatrix} \text{ belongs to } \bar{\mathcal{Y}}, \text{ so does } \begin{bmatrix} -\bar{\sigma}_{11} & -\bar{\sigma}_{12} & \bar{\sigma}_{13} \\ -\bar{\sigma}_{21} & -\bar{\sigma}_{22} & \bar{\sigma}_{23} \\ \bar{\sigma}_{31} & \bar{\sigma}_{32} & -\bar{\sigma}_{33} \end{bmatrix}. \tag{5}$$

This assumption is not restrictive at all. We refer the reader to [15] and references therein for a discussion of this symmetry condition.

2.2. *Anti-plane shear.* Due to our assumptions, the two-dimensional scalar problem that corresponds to anti-plane shear is well defined. More precisely, for $i = \mathrm{f}$, $i = \mathrm{m}$ and

$i = \text{hom}$, we define the sets

$$\mathcal{Y}_i = \left\{ \sigma = (\sigma_1, \sigma_2) \in \mathbb{R}^2 : \begin{bmatrix} 0 & 0 & \sigma_1 \\ 0 & 0 & \sigma_2 \\ \sigma_1 & \sigma_2 & 0 \end{bmatrix} \in \bar{\mathcal{Y}}_i \right\}. \tag{6}$$

For each $\mathbf{x} = (x_1, x_2) \in \mathbb{R}^2$, we also define

$$\mathcal{Y}_{\mathbf{x}} = \begin{cases} \mathcal{Y}_{\mathrm{f}} & \text{if } \{\mathbf{x}\} \times \mathbb{R} \text{ is included in a fiber,} \\ \mathcal{Y}_{\mathrm{m}} & \text{if } \{\mathbf{x}\} \times \mathbb{R} \text{ is included in the matrix.} \end{cases} \tag{7}$$

We say that a two-dimensional vector field $\sigma = \sigma(\mathbf{x}) = (\sigma_1(x_1, x_2), \sigma_2(x_1, x_2))$ is admissible if it is Q-periodic, it satisfies the restrictions

$$\sigma(\mathbf{x}) \in \mathcal{Y}_{\mathbf{x}} \text{ for all } \mathbf{x} \in \mathbb{R}^2 \tag{8}$$

and the equilibrium equations

$$\nabla \cdot \sigma = 0, \tag{9}$$

where $\nabla \cdot \sigma$ is the divergence of σ in two dimensions.

It can be easily shown that, given the conditions stated in this section,

$$\mathcal{Y}_{\mathrm{hom}} = \{\tau : \tau = \langle \sigma \rangle, \text{ for some 2D admissible vector field } \sigma\}, \tag{10}$$

where $\langle \sigma \rangle$ is now the two-dimensional average of σ, i.e., $\langle \sigma \rangle = |Q|^{-1} \int_Q \sigma(\mathbf{x})\, \mathrm{d}\mathbf{x}$ with $|Q|$ being the area of Q.

All the vector fields we will consider in the rest of this paper are two-dimensional. The two-dimensional sets $\mathcal{Y}_{\mathrm{f}}$, $\mathcal{Y}_{\mathrm{m}}$ and $\mathcal{Y}_{\mathrm{hom}}$ will also be referred to as the yield sets of the fibers, the matrix and the composite, respectively.

2.3. *The yield sets of the pure phases.* We will assume that the sets $\mathcal{Y}_{\mathrm{f}}$ and $\mathcal{Y}_{\mathrm{m}}$ are circles centered at the origin with radius Y_{f} and Y_{m}, respectively. Thus, defining

$$Y_{\mathbf{x}} = \begin{cases} Y_{\mathrm{f}} & \text{if } \{\mathbf{x}\} \times \mathbb{R} \text{ is included in a fiber,} \\ Y_{\mathrm{m}} & \text{if } \{\mathbf{x}\} \times \mathbb{R} \text{ is included in the matrix,} \end{cases} \tag{11}$$

we have that a vector field σ is admissible if and only if σ is Q-periodic, $\|\sigma(\mathbf{x})\| \leq Y_{\mathbf{x}}$ for all $\mathbf{x} \in \mathbb{R}^2$ and $\nabla \cdot \sigma = 0$, where $\|.\|$ denotes the euclidean norm, i.e., $\|(z_1, z_2)\| = \sqrt{z_1^2 + z_2^2}$ for all $\mathbf{z} = (z_1, z_2) \in \mathbb{R}^2$. Note that divergence-free vector fields can be regarded as the velocity field of an incompressible fluid. Thus, in the rest of this paper, we will sometimes refer to two-dimensional divergence free vector fields as stresses and sometimes as fluid velocity fields.

3. Bound on the yield set of the composites. Given any vector $\mathbf{z} = (z_1, z_2)$ we denote by $\mathbf{z}^\perp$ the vector perpendicular to $\mathbf{z}$ that results from rotating $\mathbf{z}$ to an angle of $\pi/2$ in the counterclockwise direction $\mathbf{z}^\perp = (-z_2, z_1)$. Also, $\cdot$ denotes the dot product, i.e., $\mathbf{u} \cdot \mathbf{w} = u_1 w_1 + u_2 w_2$ for all two-dimensional vectors $\mathbf{u} = (u_1, u_2)$ and $\mathbf{w} = (w_1, w_2)$.

Observation 3.1. Let σ and α be two Q-periodic divergence-free vector fields. Then,

$$\langle \sigma \cdot \alpha^\perp \rangle = \langle \sigma \rangle \cdot \langle \alpha \rangle^\perp. \tag{12}$$

This is a known fact that we do not prove here (see [15] for details).

We will refer to the cross sections of the fibers as the inclusions. In other words, the inclusions are the connected components of the set $\{\mathbf{x} \in \mathbb{R}^2 : Y_{\mathbf{x}} = Y_{\mathrm{f}}\}$.

ASSUMPTION 3.2. For any inclusion I, we will assume in the rest of this paper that the number of points that belong to the boundary of I and also to the boundary of an other inclusion is finite.

OBSERVATION 3.3. Let I be an inclusion and P_I its perimeter, i.e., P_I is the length of the boundary of I. If σ and α are two admissible vector fields, then

$$\left| \int_I \sigma(\mathbf{x}) \cdot \alpha^{\perp}(\mathbf{x}) \, \mathrm{d}\mathbf{x} \right| \leq \frac{1}{2} \left(Y_{\mathrm{m}} P_I \right)^2 . \tag{13}$$

Proof. We first note that, since σ and α are divergence-free, there exist $\psi = \psi(\mathbf{x})$ and $\phi = \phi(\mathbf{x})$, two scalar functions defined in $\mathbb{R}^2$, such that

$$\sigma = (\nabla \psi)^{\perp} \text{ and } \alpha = (\nabla \phi)^{\perp} , \tag{14}$$

where $\nabla\psi$ and $\nabla\phi$ are the gradients of ψ and ϕ, respectively. Using this last equation, the divergence theorem, the fact that the dot product of two vectors does not change if we rotate the two vectors by the same angle, and the fact that $(\mathbf{z}^{\perp})^{\perp} = -\mathbf{z}$ for all vectors $\mathbf{z}$, we obtain

$$\begin{aligned} \int_I \sigma \cdot \alpha^{\perp} \, \mathrm{d}A = - \int_I (\nabla \psi)^{\perp} \cdot \nabla \phi \, \mathrm{d}A = - \int_{\partial I} \phi \, (\nabla \psi)^{\perp} \cdot \hat{n} \, \mathrm{d}\ell \\ = \int_{\partial I} \phi \, \nabla \psi \cdot \hat{n}^{\perp} \, \mathrm{d}\ell, \end{aligned} \tag{15}$$

where ∂I is the boundary of I and $\hat{n} = \hat{n}(\mathbf{x})$ is the vector of norm one perpendicular to ∂I at $\mathbf{x}$ that points outward I. In the above integrals, we have used the notation $\mathrm{d}A$ for area integrals and $\mathrm{d}\ell$ for line integrals.

Let $\mathbf{x} = \mathbf{x}(s)$ be a parametrization of ∂I in the counterclockwise direction. Let $\mathbf{x}'(s)$ be the derivative of $\mathbf{x}(s)$ with respect to s. We assume that ∂I is regular enough so that the parametrization $\mathbf{x}(s)$ can be chosen to satisfy $\|\mathbf{x}'(s)\| = 1$ for all $0 \leq s \leq P_I$ except probably in a finite number of points s where $\mathbf{x}'(s)$ is not defined. Thus, it is easy to verify that the following is true:

$$\hat{n}^{\perp}(\mathbf{x}(s)) = \mathbf{x}'(s) \tag{16}$$

and

$$\phi(\mathbf{x}(s)) = \phi(\mathbf{x}(0)) + \int_0^s \nabla \phi(\mathbf{x}(t)) \cdot \mathbf{x}'(t) \, \mathrm{d}t. \tag{17}$$

Using the last three equations, we obtain

$$\begin{aligned} \int_I \sigma \cdot \alpha^{\perp} \, \mathrm{d}A = \int_0^{P_I} \left(\phi(\mathbf{x}(0)) + \int_0^s \nabla \phi(\mathbf{x}(t)) \cdot \mathbf{x}'(t) \mathrm{d}t \right) \nabla \psi(\mathbf{x}(s)) \cdot \mathbf{x}'(s) \, \mathrm{d}s \\ = \int_0^{P_I} \nabla \psi(\mathbf{x}(s)) \cdot \mathbf{x}'(s) \left(\int_0^s \nabla \phi(\mathbf{x}(t)) \cdot \mathbf{x}'(t) \, \mathrm{d}t \right) \mathrm{d}s. \end{aligned} \tag{18}$$

Note that Assumption 3.2 implies that, for all $s \in [0, P_I]$ except probably a finite set, $\mathbf{x}(s)$ is in the boundary of the interior of the matrix. Using this fact, equations (14) and (16), the fact that σ is admissible, and the fact that the value of $\sigma \cdot \hat{n}$ at the inclusion boundary is the same in the inclusion side as in the matrix side, we get

$$|\nabla\psi(\mathbf{x}(s)) \cdot \mathbf{x}'(s)| = |\sigma(\mathbf{x}(s)) \cdot \hat{n}(\mathbf{x}(s))| \leq \|\sigma(\mathbf{x}(s))\| \leq Y_{\mathrm{m}}. \tag{19}$$

Similarly, $|\nabla\phi(\mathbf{x}(t)) \cdot \mathbf{x}'(t)| \leq Y_{\mathrm{m}}$. Thus, going back to equation (18), we obtain

$$\begin{aligned}\left|\int_I \sigma \cdot \alpha^\perp \,\mathrm{d}A\right| &\leq \int_0^{P_I} |\nabla\psi(\mathbf{x}(s)) \cdot \mathbf{x}'(s)| \left(\int_0^s |\nabla\phi(\mathbf{x}(t)) \cdot \mathbf{x}'(t)| \,\mathrm{d}t\right) \mathrm{d}s \\ &\leq (Y_{\mathrm{m}})^2 \int_0^{P_I} \left(\int_0^s \mathrm{d}t\right) \mathrm{d}s = \frac{1}{2}\left(Y_{\mathrm{m}} P_I\right)^2, \end{aligned} \tag{20}$$

which proves the validity of equation (13). □

The period cell Q is a parallelogram and thus, there are two vectors $\mathbf{u}, \mathbf{w} \in \mathbb{R}^2$ such that

$$Q = \left\{\mathbf{x} \in \mathbb{R}^2 : \mathbf{x} = s\mathbf{u} + t\mathbf{w} \text{ for some } 0 \leq s < 1 \text{ and } 0 \leq t < 1\right\}. \tag{21}$$

We say that two inclusions I_1 and I_2 are equivalent if there exists integers k and ℓ such that $I_2 = I_1 + k\mathbf{u} + \ell\mathbf{w}$. We denote by $\mathbb{I}$ a set of inclusions that contains exactly one inclusion per equivalent class. We will need the set $\mathbb{I}$ when we take averages. For example, one choice of $\mathbb{I}$ is the set of inclusions whose center of mass is in Q.

Observation 3.4. Let ν be the volume fraction of the inclusions, i.e.,

$$\nu = \frac{|\{\mathbf{x} \in Q \text{ and } \mathbf{x} \in \text{an inclusion}\}|}{|Q|}, \tag{22}$$

where we are denoting the area of any two-dimensional set A by $|A|$.

We define the parameter

$$\eta = \max_{I \text{ inclusion}} \frac{P_I^2}{|I|}, \tag{23}$$

where as before, P_I is the length of the boundary of the inclusion I. If σ and α are two admissible vector fields, then

$$\left|\langle\sigma\rangle \cdot \langle\alpha\rangle^\perp\right| \leq (1-\nu)\, Y_{\mathrm{m}}^2 + \frac{1}{2}\nu\eta Y_{\mathrm{m}}^2. \tag{24}$$

Proof. From Observations 3.1 and 3.3 it can be easily shown that

$$\left|\langle\sigma\rangle \cdot \langle\alpha\rangle^\perp\right| \leq (1-\nu)\, Y_{\mathrm{m}}^2 + \frac{Y_{\mathrm{m}}^2}{2|Q|} \sum_{I \in \mathbb{I}} P_I^2. \tag{25}$$

In the above inequality the first term is a bound of $\left|\int_{Q \cap \text{matrix}} \sigma \cdot \alpha^\perp \,\mathrm{d}A\right| / |Q|$ and the second term is a bound of $\left|\sum_{I \in \mathbb{I}} \int_I \sigma \cdot \alpha^\perp \,\mathrm{d}A\right| / |Q|$.

We use this last equation and the fact that, for all inclusions I, $P_I^2 \leq \eta |I|$, to get

$$\left|\langle\sigma\rangle \cdot \langle\alpha\rangle^\perp\right| \leq (1-\nu)\, Y_{\mathrm{m}}^2 + \frac{Y_{\mathrm{m}}^2}{2|Q|}\eta \sum_{I \in \mathbb{I}} |I|. \tag{26}$$

Equation (24) follows once we note that $\nu = |Q|^{-1} \sum_{I \in \mathbb{I}} |I|$. □

OBSERVATION 3.5. Let τ be a vector such that both τ and $\tau^{\perp}$ belong to $\mathbf{Y}_{\text{hom}}$. Then,

$$\|\tau\| \leq Y_{\text{m}} \sqrt{(1-\nu) + \frac{1}{2}\nu\eta}, \tag{27}$$

where ν is the volume fraction of the inclusions and η is as defined in equation (23).

Proof. Since both τ and $\tau^{\perp}$ belong to $\mathbf{Y}_{\text{hom}}$, there exist σ and α admissible vector fields such that $\tau = \langle\sigma\rangle$ and $\tau^{\perp} = \langle\alpha\rangle$. Applying equation (24) and taking the square root completes the proof of this observation. □

When reinforcing a material, it is usually desirable that the material is strong in all directions. Thus, it is of interest to evaluate *strength* of the weakest direction of the composite. This motivates the following definition.

DEFINITION 3.6. Let $\mathbf{e} \in \mathbb{R}^2$ be a vector of length 1. We say that the strength of the composite in the direction $\mathbf{e}$ is $S_{\mathbf{e}}$ if $t\,\mathbf{e} \in \mathbf{Y}_{\text{hom}}$ for all $t < S_{\mathbf{e}}$ and $t\,\mathbf{e} \notin \mathbf{Y}_{\text{hom}}$ for all $t > S_{\mathbf{e}}$.

Note that such $S_{\mathbf{e}}$ is well defined because $\mathbf{Y}_{\text{hom}}$ is convex and the vector $\mathbf{0}$ belongs to $\mathbf{Y}_{\text{hom}}$.

Our bound will, in fact, be a bound on the strength of the weakest direction of the composite, which we define next.

DEFINITION 3.7. The strength of the weakest direction of the composite is

$$Y_{\text{hom}}^{\text{weak}} = \inf_{\{\mathbf{e}\in\mathbb{R}^2 : \|\mathbf{e}\|=1\}} S_{\mathbf{e}}. \tag{28}$$

A little thought will convince the reader that $Y_{\text{hom}}^{\text{weak}}$ is the strength of the weakest direction of the composite. The composite can withstand stresses of norm less than $Y_{\text{hom}}^{\text{weak}}$ in all directions. On the other hand, if $t > Y_{\text{hom}}^{\text{weak}}$, there are stresses of norm t that the composite cannot withstand.

A main result of this paper, which is a direct consequence of Observation 3.5, is now stated in the following theorem.

THEOREM 3.8. The strength of the weakest direction of the composite, $Y_{\text{hom}}^{\text{weak}}$, satisfies the bound

$$Y_{\text{hom}}^{\text{weak}} \leq Y_{\text{m}} \sqrt{(1-\nu) + \frac{1}{2}\nu\eta}, \tag{29}$$

where ν is the volume fraction of the inclusions and η is as defined in equation (23).

4. Composites with circular inclusions. The square of the perimeter of a circle divided by its area is equal to 4π. Thus,

$$\eta = 4\pi \qquad \text{if all the inclusions are circular,} \tag{30}$$

where η is the parameter defined in equation (23). As a consequence, our bound (equation (29)) becomes

$$Y_{\text{hom}}^{\text{weak}} \leq Y_{\text{m}} \sqrt{(1-\nu) + 2\nu\pi} \qquad \text{if all the inclusions are circular,} \tag{31}$$

where, as before, ν is the volume fraction of the inclusions. In particular, since $0 < \nu < 1$, we have that

$$Y_{\text{hom}}^{\text{weak}} < Y_{\text{m}}\sqrt{2\pi} \qquad \text{if all the inclusions are circular.} \tag{32}$$

Note that, no matter the strength of the inclusions, if they are circular, the strength of the composite is never more than $\sqrt{2\pi}$ times the strength of the matrix (again the word "strength" is used informally but its meaning in this context should be clear). We remark that the fact that the yield set of a composite with circular inclusions is bounded independently of the yield set of the inclusions is not our discovery, it is a known fact (see [6, 24] for example).

5. Composites with slender rectangular inclusions. Our bound suggests that, to obtain strong composites, we should use inclusions that lead to a large parameter η. As illustrated in the next example, η becomes large when the inclusions are slender.

A natural choice would be to consider elliptical inclusions. However, to make the calculations easier to follow, we will assume the inclusions to be rectangular. For each inclusion I, let γ_I be the length of one of the longest sides of I divided by the length of one of the shortest sides of I. Assume that γ_I is the same value for all inclusions I. Denote this value by γ, i.e., $\gamma = \gamma_I$ for any inclusion I,

$$\gamma = \frac{\text{length of longest side of an inclusion}}{\text{length of shortest side of the same inclusion}}. \tag{33}$$

Note that, the square of the perimeter of one of these rectangular inclusions divided by its area is equal to $4(\gamma+1)^2/\gamma$,

$$\eta = \frac{4(\gamma+1)^2}{\gamma}, \tag{34}$$

where η is the parameter defined in equation (23).

To be under the assumptions of our analysis (Section 3), we assume that the boundary of two different inclusions intersects at most in one point. We are particularly interested in the limit $\gamma \gg 1$. Note that $\eta \approx 4\gamma$ for $\gamma \gg 1$. As a consequence, our bound (equation (29)) becomes

$$Y_{\text{hom}}^{\text{weak}} \leq Y_{\text{m}}\sqrt{2\nu\gamma} \text{ for } \gamma \gg 1 \text{ and } \nu > 0, \tag{35}$$

where, as before, ν is the volume fraction of the inclusions.

The natural question that our analysis raises is whether the bound of equation (35) is sharp or not. To show that the answer to this question is yes, we next construct a composite with rectangular inclusions whose weakest direction is of the order of $Y_{\text{m}}\sqrt{\nu\gamma}$.

6. Composite with slender rectangular inclusions that is strong in all directions. We start by considering the composite of Figure 1. The inclusions are in dark and the matrix in white. Each inclusion is a rectangle of width w and length ℓ, with $w \ll \ell$. The inclusions are embedded in the matrix forming the regular pattern shown in Figure 1. We denote by ε the distance between neighboring inclusions. We assume that $\varepsilon \ll w$.

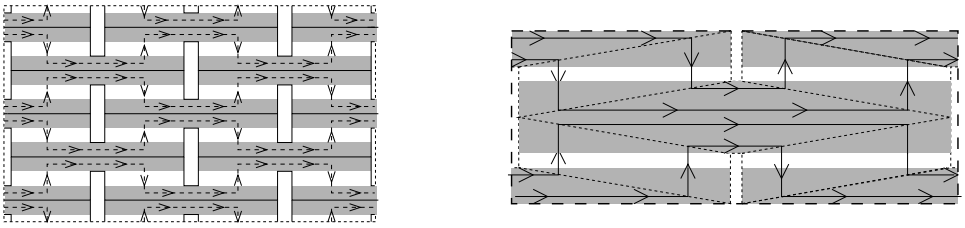

FIG. 1. Composite with rectangular inclusions and an admissible field σ described in the text.

We now construct an admissible field σ that satisfies $\langle\sigma\rangle \approx (Y_{\mathrm{m}}\ell/(2w), 0)$. Note that, as mentioned before, σ can be regarded as the velocity field of an incompressible fluid. In this context, the fact that $Y_{\mathrm{m}} \ll Y_{\mathrm{f}}$ means that fluid can flow much faster within the inclusions than in the matrix. In the left side of Figure 1, the dashed lines with arrows denote the direction of σ. Roughly speaking, fluid flows fast in the horizontal direction within the inclusions, and fluid flows slow in the vertical direction as fluid needs to go through the matrix as it flows from one inclusion to a neighboring inclusion. The details of the flow is shown in the right side of Figure 1, where we only show one full inclusion and a quarter of each of its neighboring inclusions. In the regions where fluid flows horizontally, $\sigma = (Y_{\mathrm{m}}(\ell - \varepsilon)/w, 0)$. In the regions where fluid flows vertically, $\sigma = (0, \pm Y_{\mathrm{m}})$. Note that $\sigma = 0$ inside the vertical rectangles of the left side of Figure 1 that are included in the matrix. It can be calculated that $\langle\sigma\rangle = (Y_{\mathrm{m}}(\ell - \varepsilon)/(2w + 2\varepsilon), 0)$ and thus, neglecting ε we get that,

$$\text{average velocity of the flow in Figure 1} \approx Y_{\mathrm{m}}\frac{\gamma}{2}(1, 0), \tag{36}$$

where, as defined in equation (33), $\gamma = \ell/w$. Note that we have implicitly assumed that $Y_{\mathrm{f}} \geq Y_{\mathrm{m}}\gamma$.

In Figure 2 we show a rectangular stripe of length L and width W made of the composite of Figure 1, where the dimensions of the stripe are much bigger than the dimensions of the inclusions $\ell \ll L$ and $w \ll W$, and the longest sides of the inclusions are parallel to the longest sides of the stripe. More precisely, $W = (2n + 1/2)(w + \varepsilon)$ and $L = (n + 1/2)(\ell + \varepsilon)$, where we assume $n \gg 1$. Thus,

$$\frac{L}{W} \approx \frac{\gamma}{2}, \tag{37}$$

where, as defined in equation (33), $\gamma = \ell/w$. In the example of Figure 2, $n = 3$. Following similar arguments as in the construction of the flow in Figure 1, we construct, in Figure 2, a new fluid velocity field, that we also call σ, that satisfies the constraints (8) and (9) such that: fluid enters the stripe from the left side, fluid leaves the stripe from the top side and no fluid crosses the other two sides. The rate at which fluid enters the stripe in Figure 2 is the same as if the flow was as in Figure 1. Thus, from equation (36), we have

$$\text{rate at which area of fluid enters the stripe in Figure 2} \approx Y_{\mathrm{m}}W\frac{\gamma}{2}. \tag{38}$$

In Figure 3 we construct a periodic composite. That figure shows a period cell. The stripes seen in Figure 3 are as in Figure 2, but instead of being straight rectangles, these

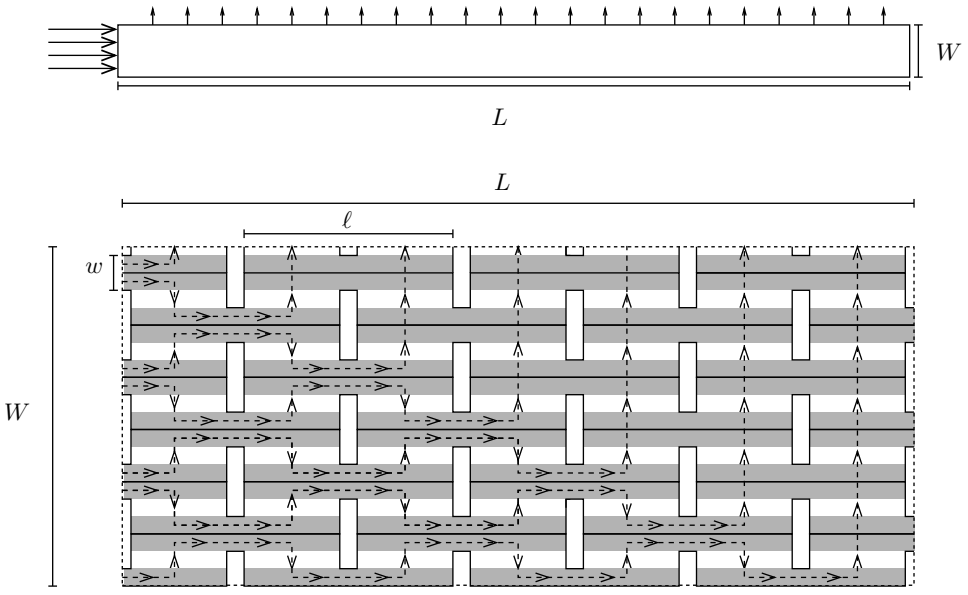

FIG. 2. Stripe made of the composite of Figure 1. Top figure, macroscopic view. Bottom figure, microscopic view. The arrows indicate the velocity field σ.

stripes are curved. Note that all of these stripes are finite in length. Note also that the inclusions are much smaller than the stripes and cannot be seen in Figure 3. To help the reader visualize this microstructure, we have shaded one of the stripes black.

Our final goal is to show that, for the composite of Figure 3, we can construct admissible fields σ that satisfy $\langle\sigma\rangle \approx (Y_{\rm m}/2)\sqrt{\gamma\nu/2}(\pm 1, \pm 1)$, where as mentioned before $\gamma = \ell/w$. This and the fact that $\mathcal{Y}_{\rm hom}$ is convex implies that, for the composite of Figure 3,

$$\mathcal{Y}_{\rm hom} \supseteq \text{ ball centered at the origin of radius } \frac{Y_{\rm m}}{2}\sqrt{\frac{\gamma\nu}{2}}. \tag{39}$$

As a consequence, for the composite of Figure 3, we have

$$Y_{\rm hom}^{\rm weak} \geq Y_{\rm m}\sqrt{\frac{\gamma\nu}{8}} \text{ for } \gamma \gg 1 \tag{40}$$

(see equation (28) for the definition of $Y_{\rm hom}^{\rm weak}$). This shows that our bound, which is equation (35) for composites with rectangular inclusions, gives the correct scaling law in terms of the parameters $Y_{\rm m}$, γ and ν.

We now proceed with the construction of the mentioned admissible fields. More precisely, we will construct an admissible field σ such that $\langle\sigma\rangle \approx (Y_{\rm m}/2)\sqrt{\gamma\nu/2}(1, 1)$ (the other fields with average $(Y_{\rm m}/2)\sqrt{\gamma\nu/2}(\pm 1, \pm 1)$ are constructed similarly).

To avoid a very crowded figure, in the left side of Figure 4 we only show two halved stripes. These two halved stripes are part of the stripes in the upper left corner of Figure 3. Even though the stripes are not rectangles, since the bending of the stripes occurs in a length scale much larger than the length of the inclusions (which are not

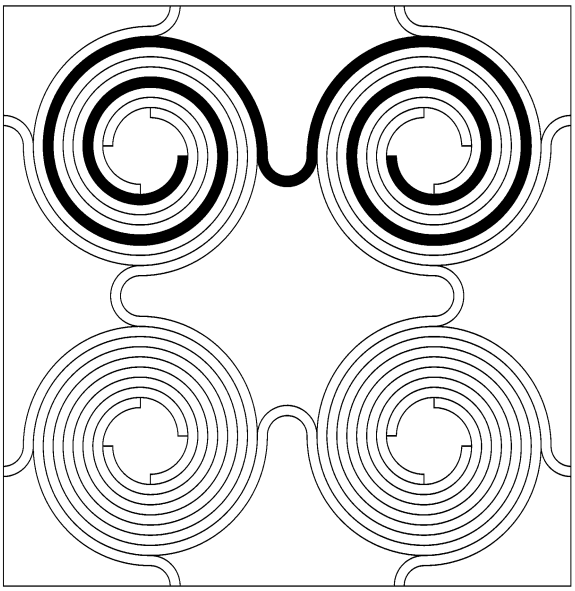

FIG. 3. Periodic composite. The stripes (both dark and white) are as in Figure 2 but curved.

seen in this figure), we can use similar arguments as in Figure 2 to construct the flow displayed in the left side of Figure 4. The arrows indicate the *average* direction of the flow when the flow is looked at in the scale of the stripes. If we were to look at the details of the flow in the scale of the inclusions, the flow would look as in the bottom part of Figure 2. Let W be the width of a stripe and L be now the length of half a stripe, from the arguments in the discussion of Figure 3, we need $W/L \leq 2w/\ell = 2/\gamma$ so that this flow satisfies the constraints (8) and (9). Thus, we will have

$$\frac{L}{W} \approx \frac{\gamma}{2}, \text{ where } L = \text{length of half a stripe and } W = \text{width of a stripe.} \tag{41}$$

In the right side of Figure 4, we show the complete upper left corner of Figure 3. The arrows indicate the *average* direction of σ. Fluid flows between neighboring stripes crossing the dashed lines. There is no flow across the solid lines. While we do not show it here, fluid flows similarly in the rest of the period cell. Fluid flows from stripe to a neighboring stripe so that, on average, fluid flows in the direction of the vector $(1,1)$.

We now compute $\langle\sigma\rangle$ for the flow of Figure 4. The period cell Q is a square. Denote by q the length of each side of Q. Simple arguments show that

$$\langle\sigma\rangle = \frac{1}{q} \times \text{ rate area of fluid enters } Q \text{ from the left } \times (1,1). \tag{42}$$

Since fluid enters through the two stripes that intersect the left side of the period cell, equation (38) implies

$$\langle\sigma\rangle \approx \frac{1}{q} Y_{\mathrm{m}} W \gamma (1,1), \tag{43}$$

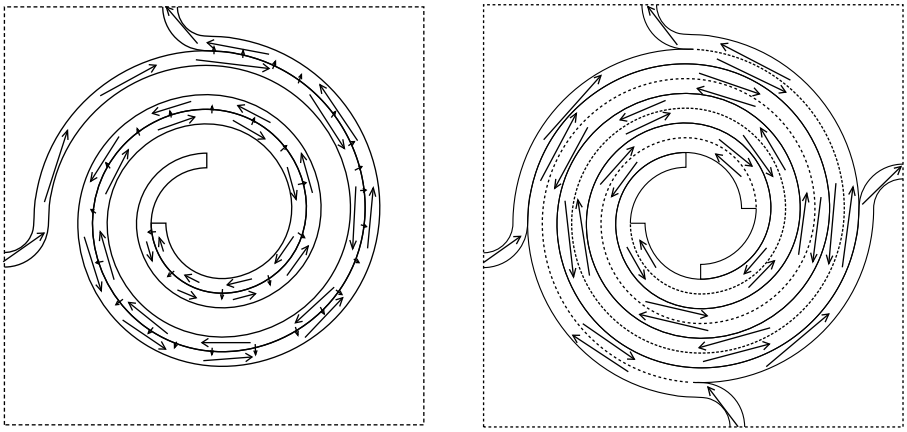

FIG. 4. Flow in the upper left corner of the composite of Figure 3. Only two halved stripes are shown in the left figure. All the stripes are shown in the right figure.

where we recall that W is the width of each stripe. Recall also that L is half the length of each stripe. In the limit in which the size of the inclusions is much smaller than the size of the stripes, we can fill most of the stripes with inclusions. Thus, since there are 4 half stripes in a quarter of the period cell, we have

$$\nu \approx \frac{16WL}{q^2}. \tag{44}$$

Finally, equations (41), (43) and (44) imply

$$\langle \sigma \rangle \approx Y_{\mathrm{m}} \sqrt{\frac{\nu\gamma}{8}}(1,1). \tag{45}$$

7. Discussion. We have introduced a bound on the strength of the weakest direction of fiber-reinforced ideally plastic composites that is valid under some symmetry conditions. This bound is a simple formula that explicitly shows the dependence of the strength of the reinforced material on the shape of the fibers and their volume fraction. We have shown with examples that this bound is optimal.

The rectangular shape of the inclusions in the examples of Sections 5 and 6 is not critical. The results remain valid if instead of rectangular we consider elliptical inclusions. The important feature needed is that the inclusions be slender. We decided to use rectangular inclusions because the calculations are easier to follow in this case.

This article has clear limitations. It is a detailed analysis on ideal scenarios that may be impossible to reproduce experimentally. The shape of cross sections of *real world* fibers are nearly circular and difficult to control. Having fibers parallel or nearly parallel to each other may also be a difficult task to produce experimentally. Thus, the predictions of this article cannot be easily verified experimentally. Additionally, we were forced to restrict our attention to anti-plane loads to reduce our problem to a two-dimensional scalar context. Our analysis cannot be easily extended beyond these restrictions.

In spite of its limitations, we believe this work is an interesting, valuable, and certainly *very novel* step toward the difficult goal of understanding the dependence of the strength of fiber-reinforced composites on the microgeometry and the properties of the fibers and of the matrix.

References

[1] A. Garroni, V. Nesi, and M. Ponsiglione, *Dielectric breakdown: optimal bounds*, R. Soc. Lond. Proc. Ser. A Math. Phys. Eng. Sci. **457** (2001), no. 2014, 2317–2335, DOI 10.1098/rspa.2001.0803. MR1862657

[2] J. F. W. Bishop and R. Hill, *A theory of the plastic distortion of a polycrystalline aggregate under combined stresses*, Philos. Mag. (7) **42** (1951), 414–427. MR0041691

[3] G. Bouchitté and P. Suquet, *Homogenization, plasticity and yield design*, Composite media and homogenization theory (Trieste, 1990), Progr. Nonlinear Differential Equations Appl., vol. 5, Birkhäuser Boston, Boston, MA, 1991, pp. 107–133, DOI 10.1007/978-1-4684-6787-1_7. MR1145747

[4] P. Ponte Castañeda, *The effective mechanical properties of nonlinear isotropic composites*, J. Mech. Phys. Solids **39** (1991), no. 1, 45–71, DOI 10.1016/0022-5096(91)90030-R. MR1085622

[5] P. Ponte Castañeda, *New variational principles in plasticity and their application to composite materials*, J. Mech. Phys. Solids **40** (1992), no. 8, 1757–1788, DOI 10.1016/0022-5096(92)90050-C. MR1190849

[6] P. Ponte Castaneda and G. deBotton, *On the homogenized yield strength of two-phase composites*, Proc. R. Soc. Lond. A **438** (1992), 419–431.

[7] P. Ponte Castaneda and P. Suquet, *Nonlinear composites*, Advances in Appl. Mech. **34** (1997), 171–302.

[8] D. Jeulin, W. Li, and M. Ostoja-Starzewski, *On the geodesic property of strain field patterns in elastoplastic composites*, Proc. R. Soc. Lond. Ser. A Math. Phys. Eng. Sci. **464** (2008), no. 2093, 1217–1227, DOI 10.1098/rspa.2007.0192. MR2386643

[9] P. de Buhan, *Lower bound approach to the macroscopic strength properties of a soil reinforced by columns*, C. R. Acad. Sci. Paris, Serie II **317** (1993), 287–293.

[10] P. de Buhan and A. Taliercio, *A homogenization approach to the yield strength of composite materials*, European J. Mech. A. Solids **10** (1991), 129–154.

[11] G. de Botton, *The effective yield strength of fiber-reinforced composites*, Internat. J. Solids Structures **32** (1995), no. 12, 1743–1757, DOI 10.1016/0020-7683(94)00203-9. MR1331003

[12] A. Garroni and R. V. Kohn, *Some three-dimensional problems related to dielectric breakdown and polycrystal plasticity*, R. Soc. Lond. Proc. Ser. A Math. Phys. Eng. Sci. **459** (2003), no. 2038, 2613–2625, DOI 10.1098/rspa.2003.1152. MR2011358

[13] Z. Hashin, *Failure criteria for unidirectional fiber composites*, J. Appl. Mech. **47** (1980), 329–334.

[14] W. Huang, *Plastic behavior of some composite materials*, J. Comp. Mat. **5** (1971), 320–338.

[15] R. V. Kohn and T. D. Little, *Some model problems of polycrystal plasticity with deficient basic crystals*, SIAM J. Appl. Math. **59** (1999), no. 1, 172–197, DOI 10.1137/S0036139997320019. MR1647809

[16] G. Li and P. Ponte Castañeda, *The effect of particle shape and stiffness on the constitutive behavior of metal-matrix composites*, Internat. J. Solids Structures **30** (1993), no. 23, 3189–3209, DOI 10.1016/0020-7683(93)90109-K. MR1252753

[17] G. W. Milton and S. K. Serkov, *Bounding the current in nonlinear conducting composites*, J. Mech. Phys. Solids **48** (2000), no. 6-7, 1295–1324, DOI 10.1016/S0022-5096(99)00083-6. MR1766404

[18] F. Murat, *Compacité par compensation: condition nécessaire et suffisante de continuité faible sous une hypothèse de rang constant* (French), Ann. Scuola Norm. Sup. Pisa Cl. Sci. (4) **8** (1981), no. 1, 69–102. MR616901

[19] T. Olson, *Improvements on taylor's upper bound for rigid-plastic composites*, Mater. Sci. Eng. A **175** (1994), 15–20.

[20] W. Prager, *Plastic failure of fiber reinforced materials*, J. Appl. Mech. **36** (1969), 542–544.

[21] G. Sachs, *Zur ableitung einer fleissbedingun*, Z. Ver. Dtsch. Ing. **72** (1928), 734–736.

[22] L.S. Shu and B.W. Rosen, *Strength of fiber-reinforced composites by limit analysis methods*, J. Composite Mater. **1** (1967), 366–381.

[23] P. Suquet, *Analyse limite et homogénéisation* (French, with English summary), C. R. Acad. Sci. Paris Sér. II Méc. Phys. Chim. Sci. Univers Sci. Terre **296** (1983), no. 18, 1355–1358. MR720280
[24] P.-M. Suquet, *Overall potentials and extremal surfaces of power law or ideally plastic composites*, J. Mech. Phys. Solids **41** (1993), no. 6, 981–1002, DOI 10.1016/0022-5096(93)90051-G. MR1220788
[25] D. R. S. Talbot and J. R. Willis, *Variational principles for inhomogeneous nonlinear media*, IMA J. Appl. Math. **35** (1985), no. 1, 39–54, DOI 10.1093/imamat/35.1.39. MR820896
[26] L. Tartar, *Compensated compactness and applications to partial differential equations*, Nonlinear analysis and mechanics: Heriot-Watt Symposium, Vol. IV, Res. Notes in Math., vol. 39, Pitman, Boston, Mass.-London, 1979, pp. 136–212. MR584398
[27] L. Tartar, *The compensated compactness method applied to systems of conservation laws*, Systems of Nonlinear Partial Differential Equations (J.M. Ball, ed.), 1983, pp. 263–285.
[28] G. Taylor, *Plastic strains in metals*, J. Inst. Metals **62** (1938), 307–324.
[29] S. Kozlov V. Jikov and O. Oleinik, *Homogenization of differential operations and integral functionals*, Springer-Verlag, New York, 1994.
[30] V. Nesi, V. P. Smyshlyaev, and J. R. Willis, *Improved bounds for the yield stress of a model polycrystalline material*, J. Mech. Phys. Solids **48** (2000), no. 9, 1799–1825, DOI 10.1016/S0022-5096(99)00100-3. MR1765196
[31] J.R. Willis, *The overall elastic response of composite materials*, J. Appl. Mech. **50** (1983), 1202–1209.